Closing the loop

Novel quantitative fMRI approach for manipulation of the sensorimotor loop in tremor

Sharifi, S.; Luft, F.; de Boer, L.; Buijink, A. W.G.; Mugge, W.; Schouten, A. C.; Heida, T.; Bour, L. J.; van Rootselaar, A. F.

Important note
To cite this publication, please use the final published version (if applicable).
Please check the document version above.

Closing the loop: Novel quantitative fMRI approach for manipulation of the sensorimotor loop in tremor

S. Sharifi [a,d,*], F. Luft [b,d], L. de Boer [a], A.W.G. Buijink [a,d], W. Mugge [c], A.C. Schouten [c], T. Heida [b], L.J. Bour [a], A.F. van Rootselaar [a,d]

[a] Department of Neurology and Clinical Neurophysiology, Amsterdam UMC, Amsterdam Neuroscience, University of Amsterdam, Meibergdreef 9, D2-113, P.O. Box 22660, Amsterdam 1100 DD, the Netherlands
[b] Department of Biomedical Signals and Systems, TechMed Centre, University of Twente, Enschede, the Netherlands
[c] Faculty of Mechanical, Maritime and Materials Engineering, Department of Biomechanical Engineering, Delft University of Technology, Delft, the Netherlands
[d] BIC Brain Imaging Center, Academic Medical Center, Amsterdam, the Netherlands

ARTICLE INFO

ABSTRACT

Tremor is thought to be an effect of oscillatory activity within the sensorimotor network. To date, the underlying pathological brain networks are not fully understood. Disentangling tremor activity from voluntary motor output and sensorimotor feedback systems is challenging. To better understand the intrinsic sensorimotor fingerprint underlying tremor, we aimed to disentangle the sensorimotor system into driving (motor) and feedback/compensatory (sensory) neuronal involvement, and aimed to pinpoint tremor activity in essential tremor (ET) and tremor-dominant Parkinson's disease (PD) with a novel closed-loop approach.

Eighteen ET patients, 14 tremor-dominant PD patients, and 18 healthy controls were included. An MR-compatible wrist manipulator was employed during functional MRI (fMRI) while muscle activity during (in)voluntary movements was concurrently recorded using electromyography (EMG). Tremor was quantified based on EMG and correlated to brain activity. Participants performed three tasks: an active wrist motor task, a passive wrist movement task, and rest (no wrist movement).

The results in healthy controls proved that our experimental paradigm activated the expected motor and sensory networks separately using the active (motor) and passive (sensory) task. ET patients showed similar patterns of activation within the motor and sensory networks. PD patients had less activity during the active motor task in the cerebellum and basal ganglia compared to ET and healthy controls. EMG showed that in ET, tremor fluctuations correlated positively with activity in the inferior olive region, and that in PD tremor fluctuations correlated positively with cerebellar activity.

Our novel approach with an MR-compatible wrist manipulator, allowed to investigate the involvement of the motor and sensory networks separately, and as such to better understand tremor pathophysiology. In ET sensorimotor network function did not differ from healthy controls. PD showed less motor-related activity. Focusing on tremor, our results indicate involvement of the inferior olive in ET tremor modulation, and cerebellar involvement in PD tremor modulation.

1. Introduction

Tremor disorders, including essential tremor (ET) and Parkinson's disease (PD), are common and have a negative impact on quality of life (Louis and Machado, 2015). Overlapping symptoms and limited diagnostic tools can result in misdiagnosis (Jain et al., 2006; Schrag et al., 2000), especially in doubtful cases and early disease stages (Jain et al., 2006; Rizzo et al., 2016). Although challenging, understanding and comparing underlying tremor pathophysiologies is crucial and may enable an earlier diagnosis. Many studies have indicated involvement of the sensorimotor (cerebello-thalamo-cortical) network in several tremor disorders, irrespective of the underlying pathophysiological mechanisms (Gallea et al., 2015; Helmich et al., 2011; Sharifi et al., 2014). For different tremor disorders however, different areas within the network seem to play a pivotal role. The olivo-cerebellar network is thought to play an important role in tremor generation in ET (León et al., 2021; Sharifi et al., 2014), whereas changes in the basal ganglia and its interaction with the cerebello-thalamo-cortical circuit may lead to tremor in PD (Dirkx and Bologna, 2022). These findings suggest that different

brain activation patterns within the sensorimotor network specific to these disorders are likely present, possibly leading to an intrinsic sensorimotor "fingerprint" per tremor disorder.

Tremor is thought to be an effect of alterations within the sensorimotor network, where efferent motor activity and sensory feedback are tightly linked (Bucher et al., 1997). As yet, it has proven difficult to separate activity related to voluntary motor output and sensorimotor feedback mechanisms, and to pinpoint a pathological neuronal origin. Especially in ET differentiation of tremor activity from normal sensorimotor brain activity is challenging because of the co-occurrence of tremor and voluntary movement with overlapping brain networks. But also, in PD during rest tremor, neuronal activity due to afferent sensory input and activity associated with tremor are not easily differentiated. Additionally, although previous studies have led to more insight into the pathophysiology of tremor in both groups, results are heterogeneous and overlap (van der Stouwe et al., 2020). Varying inclusion criteria, including phenotypical heterogeneous groups with possible different pathophysiology, especially in ET, are thought to play an important role in the heterogeneous results (Holtbernd and Shah, 2021). Furthermore, only a very limited number of studies have directly compared brain activations between ET and Parkinsonian tremor (Li et al., 2020; Novaes et al., 2021; Rowland et al., 2015). One reason might be that tremor types, namely action tremor in ET and rest tremor in PD, hamper direct comparison in a task design.

To gain insight in the intrinsic sensorimotor fingerprints in tremor disorders, we aimed to separately identify the efferent motor network and the afferent sensory network using external perturbations. The sensorimotor system can be considered a closed-loop system. The closed-loop approach is a well-known approach in biomechanics, helping to identify the dynamics of the system by using a simplified-model (Schouten and Mugge, 2018). Inside the closed-loop sensorimotor system, different feedback loops of the central nervous system can be distinguished (Schouten and Mugge, 2018). External perturbations can be used to investigate a closed-loop system. This would give the opportunity to study the properties within the sensorimotor loop. We hypothesized that the application of controlled external perturbations during functional brain imaging allows for identification of disease-specific brain activations.

The current proof-of-principle study is to determine the potential of our closed-loop approach using a custom-made MR-compatible wrist manipulator (Bode et al., 2017; Vlaar et al., 2016) during fMRI while measuring (in)voluntary movement with electromyography (EMG). First, to validate our approach, we studied healthy individuals during two conditions controlled by the wrist manipulator. The conditions include an active motor task, thus activating the sensorimotor network, and a passive sensory task, to trigger the sensory network. Our second aim was to investigate differences in brain activations related to an active motor task and passive sensory perturbation in ET and PD, and compared to healthy controls. Our third aim was to identify specific tremor-related regions per group using EMG to indicate tremor fluctuation.

2. Materials and methods

2.1. Participants

Three groups of participants (ET, tremor dominant PD and healthy controls) were included in this study. The monocenter study was conducted at the Amsterdam UMC, location Academic Medical Center. All participants were 18 years of age or older and right hand dominant. The ET patients were diagnosed according to criteria defined by the Tremor Investigation group (Bain et al., 2000). Eighteen propranolol-sensitive ET patients were included, with familial bilateral postural arm tremor. Tremor severity was assessed using the TETRAS scale (Elble et al., 2012). Fourteen PD patients with rest tremor were included and were diagnosed without severe motor fluctuations and severe dyskinesia, accord-

ing to the UK Brain Bank Criteria (Bain et al., 2000). Tremor severity was assessed using the UPDRS scale part III (Goetz et al., 2008). All clinical evaluations were recorded on video and scored blindly by an experienced neurologist. To rule out the effects of medication, both groups were asked to temporarily stop or reduce anti-tremor medication at least three days before recording according to individualized schemes. Furthermore, eighteen healthy controls with no history of familial tremor or neurological disorders participated. The study protocol was approved by the medical–ethical board of the Academic Medical Center, Amsterdam, according to the Declaration of Helsinki. Informed written consent was obtained from each subject prior to participation. Seven participants (three ET patients, one PD patient, and three healthy controls) were excluded because of technical issues, leaving 15 ET patients, 13 PD patients and 15 healthy controls for final analyses. For more details, see Table 1.

2.2. Experimental protocol

Participants performed tasks in the MR scanner with their right hand. The tasks in the MRI were performed using an MR-compatible wrist manipulator (details described below). Participants were asked to hold the handle of the manipulator which was attached to the scan table (Fig. 1). The task included three conditions: (1) an active motor (sensorimotor) task: an intentional isometric motor task performed by counteracting the movement induced by the wrist manipulator; (2) a passive (sensory) movement task undergoing the movement induced by the wrist manipulator, resulting in mainly sensory input; and (3) rest, without any wrist movement or activity. All tasks were explained, demonstrated and practiced before scanning. During scanning, instructions projected on a screen placed behind the scanner could be seen via a mirror mounted on the head coil. Participants were presented visual cues including a black crosshair, a green circle and a red cross (Fig. 1 and supplementary material Fig. 1A). During the active task, participants were asked to apply force on the handle to keep the crosshair in the circle. During the passive task, a red cross appeared illustrating that no force was required. The conditions were tested in random order, in nine blocks and lasted 30 s each. Before the start of each condition, an instruction screen was presented that lasted for five seconds, during which the patients could become accustomed to the condition. During the tasks, muscle activity via EMG and torque were continuously monitored to measure tremor as well as to ensure correct task performance. The total duration of the recorded session was 16 min.

In healthy controls, the active motor task is supposed to mainly activate the motor network, but inevitably, it will also activate the sensory network (includes sensory feedback). Passive movement, thus without intentional movement or force, is expected to mainly activate the sensory network (no intentional motor output). Consequently, the experiment was set up to identify sensorimotor activity (by comparing an active motor task to rest), sensory activity (by comparing a passive task to rest), and isolated motor activity (by comparing an active task to a passive task). Comparisons between groups per contrast allow for further identification of disease-specific brain activations. In addition, tremor was measured with EMG. A tremor derivative embedded in a task design as a variable, helps to pinpoint brain activations specifically related to involuntary tremor, as described previously (Buijink et al., 2015b; Dirkx et al., 2016), and explained in more detail below.

2.3. Data acquisition

2.3.1. fMRI recordings

Blood oxygenation level-dependent (BOLD) images were acquired with a 3T MRI (Achieva, Amsterdam) and SENSE 16-channel head receive coil. The functional acquisitions consisted of a gradient echo planar T2*–weighted EPI sequence (echo time 30 ms; repetition time 2 s; flip angle 70°; field of view: 224×224 mm; voxel size 3.5 mm³). Thirty-nine axial slices covering the entire brain and cerebellum were obtained

Table 1
Age and gender overview of the participants included for analyses.

Group	Age (y)	Number Male/female	Disease duration (y)	TETRAS	UPDRS (part III)
Essential tremor	59.6 (18.2)	11/4	28 (18.2)	19.4 (8.0)	–
Parkinson's disease	64.2 (11.4)	9/4	5.2 (2.0)	–	16.1 (7.2)
Healthy controls	55.4 (13.1)	8/7	–	–	–

Categorical data are presented as number of patients and continuous data as mean(std), y year.
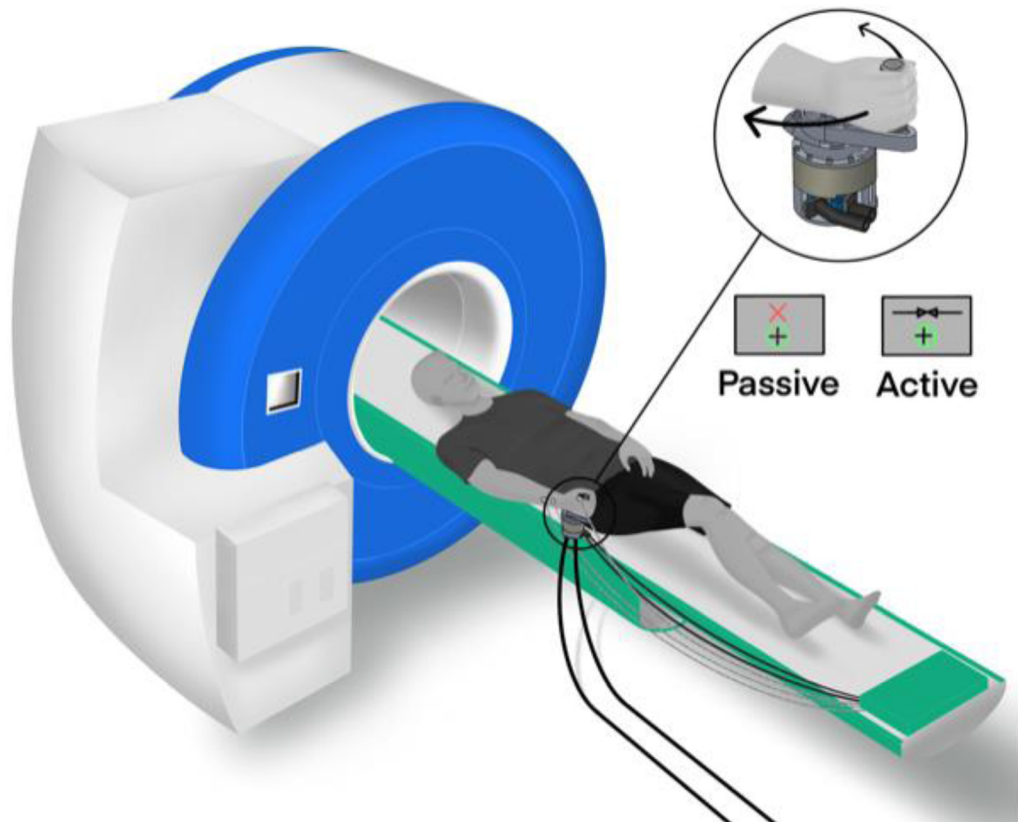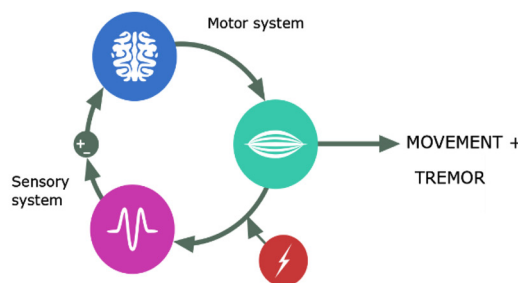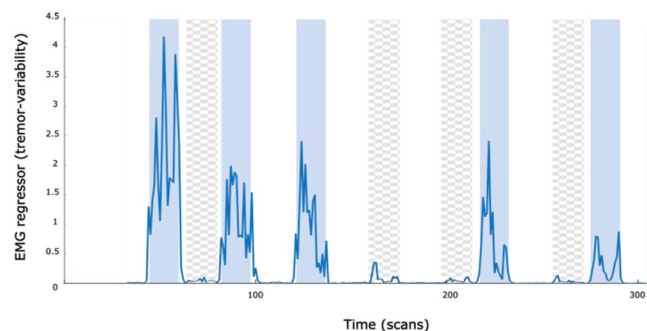
Fig. 1. (A) Schematic representation of the experimental setup. The participants were positioned inside the bore of an MRI scanner with their right hand around to the handle of the manipulator. Through a mirror located on the head coil, the participants watched the visual instructions projected on the projection screen. In the passive task, the red cross indicated that no torque was required. The green circle and black crosshairs were static during the task. In the active task, the participants were asked to apply torque to keep the black crosshair inside the green circle. The black crosshair indicated the exerted torque level by moving, thus providing visual feedback. (B) Schematic visualization of the closed loop approach, disentangling the motor efferent activity from the sensory afferent feedback by manipulating the motor and sensory system separately. (C) An illustrative example of EMG regressor representing tremor variability during different tasks in an ET patient (active task: blue line against solid blue background; passive task: blue line against checkered gray background; rest: blue line against solid white background), as a function of time. For visualization purposes, we only demonstrated a selection of 13 blocks (of a total of 27).

for a total of 520 vol. In addition, a high–resolution anatomical T1-weighted scan of the entire brain was obtained (echo time 3.64 ms; repetition time 9 ms; flip angle 8°; field of view 256 × 256 mm; voxel size 1 mm^3; number of slices 170). Foam padding was used to stabilize the head and reduce head movement during the performance of the tasks.

2.3.2. Wrist manipulator and EMG

A dedicated MR–compatible wrist manipulator was developed to apply external perturbations inducing sensory input and motor output (Delft University of Technology, Delft, Netherlands and Moog Inc, Nieuw-Vennep, Netherlands). Technical specifications have been published elsewhere (Bode et al., 2017; Vlaar et al., 2016). The device is MR-compatible and controlled using MATLAB (Mathworks Inc., Natick, MA, USA). The handle was connected to an electromotor via hydraulic tubes and optic fiber cables. The electromotor and the computer were positioned in the control room (Fig. 1 and supplementary material Figs. 2A, and 3A). Optic fiber cables measure the position and torque of the handle by registering the amount of light reflected. (Multi)sinusoidal perturbations were applied. During the tasks, EMG was recorded from three muscles of the right lower arm (the extensor carpi ulnaris, the flexor carpi radialis, and the first dorsal interosseous muscles) using braided wires to reduce the differential magnetic field effect on the EMG cables (Goldman et al., 2000) and an MR-compatible amplifier (Refa8, Twente Medical Systems International B.V., Oldenzaal the Netherlands).

2.4. fMRI and EMG pre-processing

The fMRI data was analyzed with the statistical parametric mapping software, SPM12 (Wellcome Department of Cognitive Neurology, UCL, London, UK; https://www.fil.ion.ucl.ac.uk/spm/) (Friston et al., 1995) including standardized pre-processing steps containing realignment, slice-timing, coregistration and normalization to MNI space. The scans were then spatially smoothed with an isotropic 8-mm full-width at half maximum (FWHM) Gaussian kernel. For each recording head movement were examined. Participants with more than 2 mm translation in x, y or z direction, or 1° rotation in pitch, roll and jaw axes between subsequent images were discarded.

First, to investigate the influence of the tasks on the sensorimotor network we used an explicit descriptive *task block design*; the two movement conditions (active and passive) were included as was rest. Additionally, the instruction blocks (5 s) of the active and passive wrist movement conditions were added to the design separately (supplementary material Fig. 4A). Because of a motor task-based design we included a more extensive set of movement parameters as regressors in addition to the task (Caballero-Gaudes and Reynolds, 2017; Power et al., 2013). The movement parameters included the realignment parameters, squared realignment regressors, and the global (mean) signal including their first temporal derivatives (in total 26 additional movement regressors). Global signal regression (GSR) was included in order to remove effects of nuisance contributors (Liu et al., 2017; Power et al., 2015), especially interested in brain regions that are notoriously difficult to detect with fMRI because of its size and anatomical location close to major arteries and pulsatile cerebrospinal fluid filled space, making them prone to artefacts (Beissner et al., 2014; Brooks et al., 2013). For this reason, including GSR was considered to be more useful than negatively affecting the results (Murphy and Fox, 2017).

Second, to investigate the BOLD activations related to tremor modulation a second design was used, referred to as *tremor block design* (supplementary material Fig. 5A). In this design, we added the measure for measure representing tremor derived from EMG, in addition to the task and movement parameters. EMG signals were corrected for MR artefacts using the MR-artefact correction algorithm FARM (fMRI artefact reduction for motion) (van der Meer et al., 2010). EMG was band-pass filtered (zero phase, between 52 and 570 Hz, fourth order Butterworth filter) and full-wave rectified. For each participant the optimal EMG channel was selected showing the highest and most distinct peak in power

spectral density related to tremor (around known tremor frequency and clearly above average power level). EMG was further processed to be used as a regressor by calculation of the average EMG power in a 5-Hz band around the peak tremor frequency for each scan (TR) per patient (Buijink et al., 2015b). For the ET and PD group the EMG regressor was orthogonalized with respect to the active and rest blocks, respectively, then normalized, and finally convolved with the canonical hemodynamic response function. The orthogonalized EMG regressor that is derived using Gram-Schmidt orthogonalization, maintains additional information (relating to tremor fluctuations) other than the task since it is a vector relative to the mean EMG across the task (Buijink et al., 2015b; Van Rootselaar et al., 2008). Finally, we related brain activations resulting from EMG fluctuations (reflecting the tremor) to overall clinical severity. For this, we used the entire EMG recorded during scanning, including both rest and action tremor, to derive the tremor regressor. The resulting maps for each patient were correlated with the clinical severity (TETRAS or UPDRS III) per patient group.

2.5. Statistical analysis

For each participant, the first-level General Linear Model (GLM) provided a conventional task block design, including the active task (mainly activating the motor efferent network), the passive task (activating the sensory afferent network), and rest. Further, the GLM included two instruction tasks (both the active and the passive task) and movement parameters (supplementary material Fig. 4A). First-level contrasts were designed to test for the involvement of the sensorimotor network within the effects of interest. The contrasts included the motor task vs. rest, the passive task vs. rest and the motor task vs. the passive task (the latter to investigate more isolated motor activity). The difference between the BOLD observations were calculated for each contrast, resulting in three samples for each comparison (active>rest, passive>rest and active>passive).

For the second level within group and between group comparisons, we performed non-parametric permutation procedures, not assuming a particular distribution (Statistical Non-Parametric Mapping SnPM13.1.08, http://nisox.org/Software/SnPM13/, 10.000 permutations)(Nichols and Holmes, 2002). The FWE rate was controlled using non-parametric tests and its maximum statistics. Within-group effects were tested with one-sample t-tests, with single subjects as input for every contrast. All within-group activations were reported for voxels detected at FWE corrected p value < 0.05 (if exceeding voxel>1). To specifically test the sensorimotor network and its associated areas, activation maps were masked with a sensorimotor mask using the anatomy toolbox (Eickhoff et al., 2007) (including primary motor cortex, primary somatosensory cortex, sensorimotor association areas (premotor cortex (Brodmann area 6) and secondary sensory areas (operculum), cerebellum (anterior lobe and lobule VIII), basal ganglia and thalamus; supplementary Fig. 6A). For between-group analyses, we performed two-sample t-tests using small volume correction. Because BOLD activities were expected to be weaker and limited to the hypothesized "tremor network", small volume correction was performed using the sensorimotor cerebral cortex (25,244 voxels), basal ganglia (2264 voxels), bilateral cerebellar lobules V–VIII (4330 voxels), bilateral dentate nuclei (394 voxels), and the inferior olive nucleus (206 voxels). Activations were considered significant at a threshold of FWE corrected $p < 0.05$. All activation maps were identified using the Automated Anatomical Labeling extension (AAL labeling) included in SPM12 (Rolls et al., 2020). With respect to the tremor block design (supplementary Fig. 5A), that investigated the association of BOLD activation with tremor modulation, statistical tests were performed in a similar manner. In addition, in case of investigation of tremor-related areas (with additional EMG in the block design), we applied an additional practical approach which is less stringent than the FWE method to decrease the chance of false negatives, as the cerebellum is highly associated with tremor and withholds small areas in which functions might overlap with the task. Therefore,

Table 2

Local maxima of the three contrasts in healthy controls.

Healthy controls		MNI coordinates			Statistical tests		
Brain region		X	Y	Z	T	P_{FWE}	Cluster size
Active>rest							
L	Precentral/postcentral gyrus (M1/S1)	−36	−34	59	18.54	0.0001	4666
	Precentral gyrus (M1)	−52	6	35	9.82	0.0005	274
R	Cerebellum lobules IV-V	20	−52	−19	12.12	0.0001	516
	Cerebellum lobule VIII	20	−62	−51	11.04	0.0001	477
	Precentral gyrus (M1)	50	8	43	9.68	0.0005	508
	Precentral	60	10	15	6.41	0.0099	12
	Inferior parietal lobule	42	−34	47	8.18	0.0013	435
	Operculum	46	−26	19	8.76	0.0009	196
Passive>rest							
L	Postcentral/precentral gyrus (S1/M1)	−30	−24	65	16.89	0.0001	1803
	Precentral gyrus (M1)	−44	0	19	5.82	0.0370	3
	Parietal operculum (SII)	−42	−34	19	10.18	0.0003	351
	Supplementary motor area	−10	−2	55	8.11	0.0013	51
	Thalamus	−16	−22	7	7.11	0.0068	49
R	Cerebellum lobules IV-V	22	−50	−21	14.55	0.0001	375
	Cerebellum lobule VIII	22	−60	−49	10.04	0.0003	183
		8	−68	−41	5.82	0.0373	3
	Operculum	40	−30	19	10.02	0.0003	64
	Supramarginal gyrus	64	−24	29	5.73	0.0401	2
Active>passive							
L	Precentral/postcentral gyrus (M1/S1)	−36	−36	57	10.92	0.0001	1746
	Precentral gyrus (M1)	−56	6	33	7.90	0.0018	162
	Supplementary motor area	−8	0	61	6.99	0.0054	100
		−16	−12	61	5.73	0.0251	8
R	Cerebellum lobule VI	26	−54	−23	7.55	0.0029	136
	Cerebellum lobule VIII	10	−70	−41	6.70	0.0065	43
		20	−62	−51	6.35	0.0103	61
	Precentral gyrus (M1)	44	−6	59	7.83	0.0022	117
		28	−6	47	5.62	0.0295	11
	Postcentral gyrus (S1)	36	−34	43	6.49	0.0088	61

All within-group activations reported are statistically significant values. Voxels were detected at FWE corrected p value < 0.05 (only reported if voxel number exceeds 1).

additional uncorrected maps of the cerebellum were analyzed with a threshold of $p < 0.001$.

3. Results

There were no participants excluded from the analysis due to excessive head movement. Participants performed the tasks correctly, as was demonstrated by the amount of torque that was shown on the monitor during tasks. First, we displayed the within-group results per group (healthy controls and tremor groups: ET and PD patients), followed by the between-group results.

3.1. Within-group results: sensorimotor task block design

3.1.1. Healthy controls

Results are summarized in Table 2 and Fig. 2. In healthy controls, BOLD activations related to the three contrasts (active>rest, passive>rest, and active>passive) were observed throughout the sensorimotor network. During the active motor task (active>rest), several widespread sensorimotor cerebral and cerebellar cortical areas were activated. The largest clusters included the primary motor cortex contralateral to the task and unilateral cerebellum (Table 2). During the passive movement task (passive>rest), mainly the primary and secondary somatosensory cortex (the supramarginal gyrus and the superior parietal lobule), supplementary motor area (SMA), thalamus and cerebellum were activated. The isolated motor contrast (active>passive) revealed more isolated motor activity than the active task (active>rest), showing contralateral precentral and less pronounced postcentral cortical and cerebellar activity.

3.1.2. Tremor groups

Results are summarized in Tables 3, 4 and Fig. 2. Related to the active motor task, in ET patients, significant activation was observed in the primary motor cortex contralateral to the movement, the SMA and basal ganglia (pallidum, putamen). The passive movement task revealed mostly activity in the sensory cortical areas and bilateral cerebellum. When comparing active movement to passive movement (active>passive), there was significant activation contralateral to the movement in the sensorimotor cortex, SMA, and basal ganglia but no cerebellar activity.

In PD patients, activations in the primary motor and sensory cortices were observed during the active motor task. Also, cerebellar activity (vermis and lobule VIII) was detected. During the passive movement task, bilateral primary cortical motor activity as well as bilateral primary and secondary sensory activity was observed. Also, bilateral cerebellar activity was detected. During the isolated motor contrast (active>passive), the global maximum was around the precentral gyrus.

3.2. Between-group results; sensorimotor tasks

Results are summarized in Table 5 and Fig. 3. Comparing ET patients to healthy controls, no differences were found in BOLD patterns related to the active motor task. Also, the BOLD activations related to the passive task (undergoing movement) did not reach significance in the regions of interest analyses at a voxel level.

PD patients showed, compared to healthy controls, decreased BOLD activities in the contralateral putamen and ipsilateral cerebellum during the active motor task. With passive movement, there was an increased contralateral cerebellar activity. Analyzing the isolated motor contrast
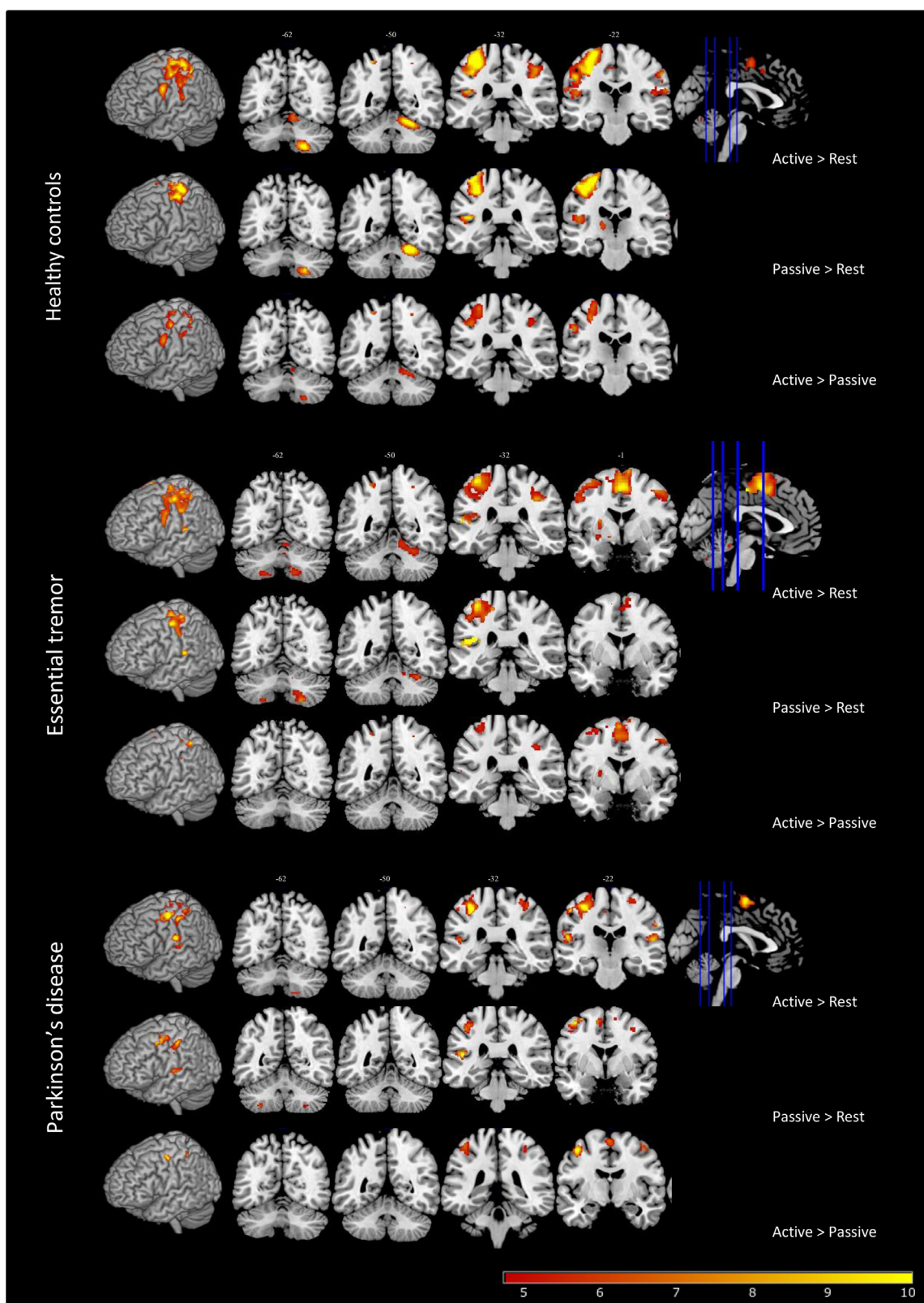
Fig. 2. Within-group results (A) active movement >rest condition; (B) Passive movement>rest condition; (C) Active>passive movement contrast. The results were depicted on the ch2-template using a sensorimotor network mask. The voxel threshold was set at FWE corrected p value < 0.05.

Table 3
Local maxima of the three contrasts in ET patients.

Essential tremor		MNI coordinates			Statistical tests		
Brain region		X	Y	Z	T	P_{FWE}	Cluster size
Active>rest							
L	Precentral/postcentral gyrus (M1/S1)/Supplementary motor area	−26	−10	57	14.12	0.0001	6231
	Pallidum	−12	0	5	7.32	0.0015	6
	Putamen	−26	−2	−13	6.97	0.0030	166
	Midbrain	−14	−14	−17	6.57	0.0050	7
	Cerebellum lobule VIII	−14	−58	−55	6.18	0.0100	98
R	Precentral gyrus (M1)	42	−4	−49	8.65	0.0005	692
	Supramarginal, postcentral gyrus	36	−34	39	9.22	0.0002	550
	Superior temporal gyrus	44	−28	15	8.10	0.0006	54
	Temporal pole: superior temporal gyrus	54	4	−3	7.32	0.0015	19
	Cerebellum lobules IV-V	10	−54	−15	6.25	0.0074	295
	Cerebellum lobule VIII	6	−70	−35	6.22	0.0077	221
Passive>rest							
L	Operculum	−38	−32	21	17.31	0.0001	394
	Postcentral/precentral gyrus (S1/M1)/Supplementary motor area	−30	−12	59	12.33	0.0001	2499
	Cerebellum lobuleVIII	−24	−66	−55	6.87	0.0122	33
R	Cerebellum lobuleVIII	24	−62	−53	7.95	0.0047	221
	Cerebellum lobules V-VI/dentate nucleus	18	−56	−25	7.03	0.0102	179
	Operculum	46	−30	17	8.85	0.0018	185
	Precentral gyrus (M1)	56	8	37	6.47	0.0179	73
Active>passive							
L	Postcentral/precentral gyrus (S1/M1)/ superior parietal lobule	−40	−42	61	10.18	0.0001	971
	Precentral gyrus (M1)	−52	2	35	5.14	0.0271	16
	Postcentral gyrus (S1)	46	−40	59	6.99	0.0019	277
	Supplementary motor area	−4	0	67	8.22	0.0003	911
	Pallidum	−14	0	−5	6.71	0.0030	2
	Putamen	−14	0	−5	6.74	0.0035	57
	Inferior parietal lobule	−56	−22	43	5.69	0.0133	15
R	Precentral gyrus (M1)	42	−6	59	7.12	0.0017	121
	Postcentral gyrus (S1)	36	−48	63	5.52	0.0160	5
	Supplementary motor area	14	−16	61	5.25	0.0233	6

All within-group activations reported are statistically significant values. Voxels were detected at FWE corrected p value < 0.05 (only reported if voxel number exceeds 1).
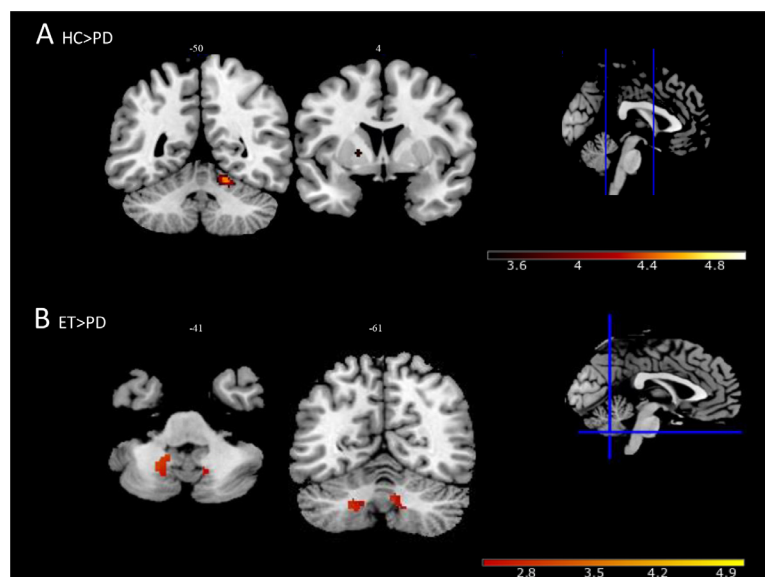
Fig. 3. Group comparison; (A) Decreased contralateral putamen and ipsilateral cerebellar activity (lobule V) in Parkinsons disease patients compared to healthy controls during the active motor task. Small volume correction, FWE corrected p value < 0.05. (B) Decreased dentate nucleus activity in Parkinsons disease patients compared to essential tremor patients during active>passive contrast. Small volume correction, FWE corrected p value < 0.05.

(active>passive) less activity was detected in the ipsilateral dentate nucleus.

PD patients showed, compared to ET patients, decreased BOLD activation in the contralateral putamen and decreased cerebellar activity during the active motor task, including decreased bilateral dentate nucleus activity. There was no significant difference found in the passive task. Analyzing the isolated motor contrast decreased bilateral activity in the dentate nuclei remained.

3.3. Tremor-related activation; tremor fluctuation based on EMG regressor

In the tremor block design, we related the tremor (EMG-)regressor with simultaneously measured brain activity. In line with the inclusion criteria, in ET patients a distinct peak in the power spectral density was present around known tremor frequency during the active task, whereas in PD patients the tremor peak was predominantly present during rest. In ET patients, the tremor regressor derived from EMG during the ac-

Table 4
Local maxima of the three contrasts in PD patients.

| Parkinson's disease		MNI coordinates			Statistical tests		
Brain region		X	Y	Z	T	P$_{FWE}$	Cluster size
Active>rest							
L	Precentral/postcentral gyrus (M1/S1)	−40	−6	57	22.75	0.0001	2577
	Postcentral gyrus (S1)	28	48	61	14.63	0.0009	260
	Supramarginal gyrus	−54	−26	15	14.06	0.0002	375
R	Operculum	58	−16	15	13.53	0.0002	190
	Supramarginal, postcentral gyrus	60	−20	33	10.08	0.0022	82
	Precentral gyrus	40	−6	49	9.81	0.0026	137
	Operculum	62	10	21	9.24	0.0037	40
	Cerebellum lobule VIII	20	−64	−53	7.01	0.0190	24
B	Vermis	6	−70	35	8.49	0.0062	9
Passive>rest							
L	Precentral gyrus (M1)	−42	6	49	11.42	0.0007	326
	Postcentral gyrus (S1)	−50	−22	49	10.14	0.0010	367
	Operculum	−44	−30	15	11.69	0.0006	448
	Supplementary motor area	−8	−4	59	7.99	0.0066	62
	Cerebellum lobule VIII	−32	−54	−51	7.04	0.0155	15
R	Precentral gyrus (M1)	46	8	35	12.69	0.0002	195
	Postcentral gyrus (S1)	62	−14	39	7.33	0.0115	48
		62	−16	17	10.58	0.0009	189
	Cerebellum Lob VIII	24	−60	−53	7.26	0.0123	33
Active>passive							
L	Precentral gyrus (M1)	−42	−6	55	11.33	0.0007	180
	Postcentral, supramarginal gyrus	−38	−42	53	9.34	0.0023	106
	Supplementary motor area	0	−6	63	7.95	0.0082	128
R	Precentral gyrus (M1)	42	−8	55	7.75	0.0104	18
	Precentral	62	8	19	6.78	0.0272	3
	Postcentral gyrus (S1)	32	−36	55	6.78	0.0271	17

All within-group activations reported are statistically significant values. Voxels were detected at FWE corrected p value < 0.05 (only reported if voxel number exceeds 1).

Table 5
Between group differences of the three contrasts.

Contrast	Groups	Brain region		X	Y	Z	T	P$_{FWE}$	P$_{uncorr}$	Cluster size
Active> Rest	ET>HC	–	–	–	–	–	–			–
	HC>ET	–	–	–	–	–	–			–
	PD>HC	–	–	–	–	–	–			–
	HC>PD	Right	Cerebellum lobule V	16	−50	−19	4.42	0.007		24
		Left	Putamen	−18	4	3	3.61	0.028		16
		Left	Dentate nucleus	−20	−52	−39	2.90	0.035		5
	ET>PD	Left	Putamen	−24	6	13	4.10	0.010		6
		Right	Cerebellum lobule V	12	−52	−15	3.21	0.041		5
		Right	Dentate nucleus	8	−66	−37	2.81	0.009		19
		Left	Dentate nucleus	−22	−56	−41	3.06	0.002		80
	PD>ET	–	–	–	–	–	–			–
Passive> Rest	HC–ET	–	–	–	–	–	–			–
	ET>HC	Left	Cerebellum lobule VIII	26	64	55	3.45	0.045		2
	PD>HC	Left	Cerebellum lobule VIII	−30	−54	−51	3.52	0.035		5
	HC>PD	–	–	–	–	–	–			–
	ET>PD	–	–	–	–	–	–			–
	ET>PD	–	–	–	–	–	–			–
	PD>ET	–	–	–	–	–	–			–
Active> Passive	HC>ET	–	–	–	–	–	–			
	ET>HC	–	–	–	–	–	–			–
	PD>HC	–	–	–	–	–	–			–
	HC>PD	Right	Dentate nucleus	8	−66	−37	2.75	0.038		10
	ET>PD	Right	Dentate nucleus	6	−62	−35	2.69	0.012		47
		Left	Dentate nucleus	−22	−60	−41	2.89	0.016		113
		Left	Cerebellum lobule VIII	−20	−54	−49	3.16	0.046		2
	PD>ET	–	–	–	–	–	–			–
Tremor	ET	Both	Inferior olive	0	−32	−51	4.00	0.003	0.0002	36
	PD	Right	Cerebellum Crus/VI	26	−76	−29	5.68	–	0.0005	60
TETRAS	ET	Right	Cerebellum lobule VIII	20	−50	−51	4.02	0.040	0.0003	1
		Left	Cerebellum lobule VIII	−22	−60	−49	4.45	0.017	0.0003	34
		Right	Dentate nucleus	16	−58	−35	3.68	0.030	0.0018	6
		Left	Dentate nucleus	−22	−60	−35	4.61	0.009	0.0002	22
	-ET	Left	Midbrain	−4	−10	−15	−5.65	–	0.0004	18
UPDRS	–	–	–	–	–	–	–			–
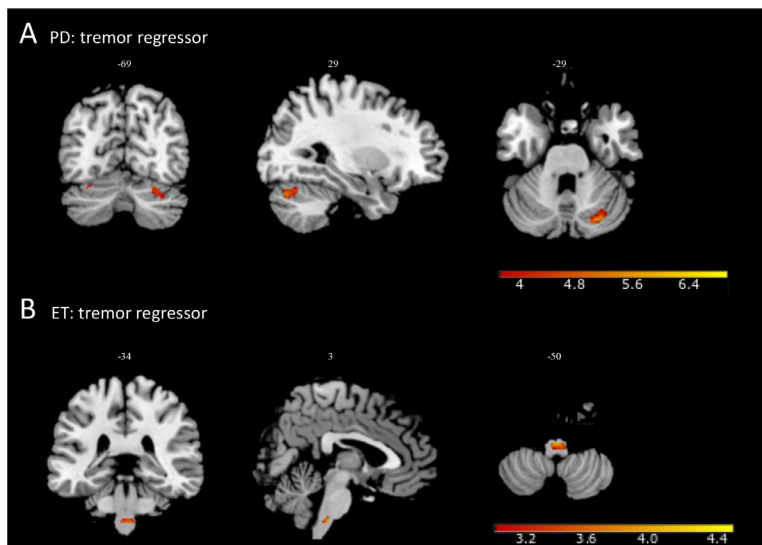
Fig. 4. Tremor-fluctuation related activation with help of EMG regressor; (A) In PD cerebellar activity (lobule crus1) correlated with the tremor-regressor. Whole brain uncorrected p value < 0.001. (B) In ET brainstem activity (inferior olive) correlated with the tremor-regressor. Small volume correction, FWE corrected p value < 0.05.
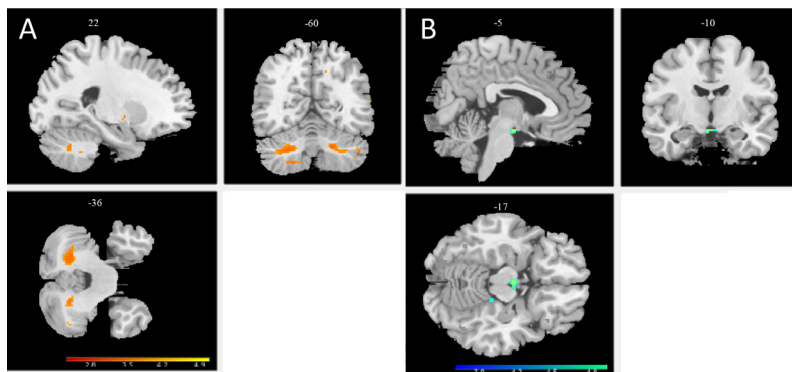
Fig. 5. Tremor-severity related activation using TETRAS score in ET; (A) Positive association between tremor severity and cerebellum. Small volume correction, FWE corrected p value < 0.05. (B) Negative correlation with tremor severity and contralateral mesencephalon. Whole brain, uncorrected p value < 0.001.

tive motor task showed a significant correlation with the inferior olive (Table 5 and Fig. 4). For the PD patients, the tremor regressor was derived from EMG during rest periods. The regressor in PD did not yield significant activity with stringent multiple comparisons correction in the regions of interest. However, analyzing regions within the cerebellum ($p < 0.001$ uncorrected), increased cerebellar activity was observed. There was a positive correlation with mainly the ipsilateral cerebellar cortex (Crus/ lobule VI).

3.4. Tremor-related activation; tremor severity based on clinical scores

For correlation with overall clinical tremor severity, we used brain regions revealed by the tremor (EMG-)regressor. In ET patients, bilateral cerebellum, including the dentate nucleus (Table 5 and Fig. 5) correlated positively with tremor severity (TETRAS). Furthermore, apart from the predefined regions of interest, the analysis showed negative correlation in the contralateral pedunculus cerebri ($p<0.001$ uncorrected). BOLD activity in the PD patients did not correlate with the UPDRS score.

4. Discussion

Our imaging study is the first to perturb the motor control and sensory loops separately using a wrist manipulator in order to investigate characteristics of the closed-loop sensorimotor system, and to assess if different tremor disorders have distinct sensorimotor fingerprints. In healthy controls, specific activations within the sensorimotor network were related to the different tasks. As expected, active motor tasks were associated with widespread activity of the contralateral sensorimotor cortices and ipsilateral cerebellar activity (Sahyoun et al., 2004;

Weiller et al., 1996). Passive movement was predominantly associated with increased widespread activity in the sensory cortices, including the primary sensory cortex, secondary cortical areas involved with somatosensory processing, the contralateral thalamus and ipsilateral cerebellum. These findings prove that, in our experimental paradigm, the sensorimotor network could be disentangled, "separating" the motor and sensory parts of the network, thereby achieving our first aim.

Differences between tremor groups for the different contrasts indicated a possible intrinsic sensorimotor fingerprint related to the specific tremor disorders. Although there is a tight communication within the sensorimotor network, it is unclear how the areas interlock and lead to tremor. With this experimental set-up, we were able to identify specific areas that have a one-to-one relation with tremor fluctuation. Between ET patients and healthy controls, sensorimotor network activations related to the wrist manipulation tasks showed no differences (no differences in 'sensorimotor fingerprint'), however tremor modulation, derived from EMG, revealed involvement of the inferior olive in ET. In PD however, the sensorimotor fingerprint is altered, showing activations which are in line with neurodegenerative anatomical changes described in literature (Armstrong and Okun, 2020). Furthermore, tremor modulation in PD seems to be associated with cerebellar involvement. Yet, we have to keep in mind the complexity of the intertwined oscillations, including pathological oscillations, in which the sensory and motor systems influence each other. This will be discussed in more detail below.

4.1. Sensorimotor fingerprint

Sensorimotor system functioning (voluntary motor output and sensory feedback) does not seem to be affected by the underlying tremor

pathophysiology in ET, as ET patients and healthy controls showed a similar pattern of brain network activations during active and passive movements. On visual inspection of the within-group analyses (Fig. 2) ET patients seem to demonstrate less cerebellar activation compared to healthy controls. However, even using exploratory statistics no differences were shown between the groups. The absence of cerebellar involvement in normal sensorimotor control in ET patients is perhaps unexpected, although not incompatible with an important role of the cerebellum in tremor facilitation/generation. Our dual task approach, with the tremor regressor in the sensorimotor design, allowed to isolate activations specifically coupled to voluntary tasks. However, previous studies in ET reported both structural and functional changes (León et al., 2021), including decreased cerebellar BOLD activation during a cerebellar finger tapping task (Buijink et al., 2015a). Cerebellar pathological oscillatory activity, might conceivably also have an effect on normal cerebellar sensorimotor functioning. In addition to the explanation above, there are several alternative explanations for the apparent discrepancies between our study and other studies. One is the specific motor task being used. Studies have shown the cerebellum in ET to react to a greater or lesser extent dependent on the type of motor tasks (Neely et al., 2015). Although speculatively, our vigorous motor task may have prevented to reveal more subtle differences beyond the task activations observed in our study. Also, increased baseline cerebellar activity (Boecker et al., 2010; Colebatch et al., 1990), would not rule out a relative lower recruitment of cerebellar activity during a motor task in the ET population compared to healthy controls.

PD showed different sensorimotor network activations compared to healthy controls and ET. The contralateral basal ganglia and ipsilateral cerebellum were less activated in the active motor task compared to both groups. Compared to ET, there was decreased bilateral dentate nucleus activity. The results are in accordance with the underlying degenerative etiology of PD, in which mainly lower cortico–striato–cerebellar interactions are observed as an effect of an overactive GABAergic subthalamic nucleus (DeLong and Wichmann, 2007; Kühn et al., 2006; Nambu et al., 2002). Also, previous imaging studies have shown hypo-activation in the basal ganglia and hypo-activation of the cerebellum during motor tasks in PD compared to ET (Neely et al., 2015; Spraker et al., 2010). Several main clinical characteristics of PD, such as resting tremor, can also contribute to differences in BOLD activation. As such, in our study, the contrast in which motor activity was compared to rest activity, could have been influenced by tremor activity during rest. This potential influence could explain the task-related decrease in relative BOLD activation observed in the cerebellum; the difference between BOLD activation during an active motor task and activity at rest might be relatively less because of a higher baseline level of BOLD activation due to tremor, which is absent in the healthy controls.

4.2. Tremor in essential tremor

The tremor regressor reveals brain activations related to tremor amplitude modulation, discarding the sensorimotor tasks in the design. In ET, inferior olive activity co-fluctuates with tremor amplitude derived from EMG. The inferior olive has been hypothesized to be a key structure in the tremor network (Boecker et al., 1996; Hallett and Dubinsky, 1993; Miwa, 2007; Park et al., 2010). However, this has recently been disputed because the evidence is mainly based on neurophysiological recordings in animal models, which may not accurately represent ET in humans (Louis and Lenka, 2017). The inferior olive, however, is notoriously difficult to study with imaging techniques because, of its size and its anatomical location, being prone to artefacts. In our experimental setup, which considered the sensorimotor task and tremor separately, we have enhanced the contrast and thereby enabled the detection of tremor-related areas. Likewise, this setup might explain the absence of cerebellar tremor-related activity as co-occuring motor task-related cerebellar activity might be regressed out. Nevertheless, our results further show tremor severity (based on clinical scores) to be associated with

increased bilateral cerebellar activation, including the dentate nucleus. The association of disinhibition of the dentate nucleus and tremor severity has previously been suggested (Buijink et al., 2015a; Gallea et al., 2015). In ET, this association may be explained by the functional disorganization of the cerebellum (perhaps secondary to faulty inferior olive activation) or by the neurodegeneration of the cerebellum. Literature has also suggested the loss of Purkinje cells as a cause of ET, as these cells have an inhibitory effect on the dentate nucleus (Louis, 2016). Also, our results show tremor severity to be negatively associated with contralateral midbrain activity. This suggests a (functional) cerebellar disconnection, whereas pathways connecting the cerebellum to the cerebrum seem to be less activated when tremor severity is increased.

Combining the above, we conclude that the sensorimotor functioning of intentional voluntary movement in ET is not different. Tremor, however, is related to olivo-cerebellar dysfunction. Whether the inferior olive activity is the pacemaker primarily leading to tremor or secondarily resulting from other cerebellar changes cannot be deduced from our study. Other structures may be involved in tremor modulation through nonlinear correlations which our linear imaging techniques will not be able to detect.

4.3. Tremor in Parkinson's disease

In PD the tremor regressor correlated with areas within the cerebellum, suggesting that the cerebellum plays a role in tremor modulation. These findings are in accordance with the "dimmer switch" hypothesis based on fMRI studies that have suggested that two systems concurrently uphold tremor. First, the faulty involvement of the basal ganglia turns on the switch to tremor, and the areas within the cerebello-thalamo-cortical network can modulate tremor intensity like a dimmer does (Dirkx et al., 2016; Helmich et al., 2011). Other modalities have also established the involvement of the cerebello-thalamo-cortical network in tremor in PD (Pollok et al., 2009; Timmermann et al., 2003). Furthermore, literature has shown that the stimulation of the dentato-rubro-thalamic tract influences tremor amplitude (Coenen et al., 2016; Prent et al., 2020). In our study, there was no significant correlation between tremor severity and the EMG regressor in the PD patients. This finding might be explained by the limited variation within the tremor-specific items in the UPDRS scores.

Interestingly, we found the function of the cerebellum and the basal ganglia to be altered in the sensorimotor task too, which may imply that dysfunction in these brain regions underlies both tremor and other sensorimotor dysfunctions.

4.4. Limitations

The experimental setup was designed to investigate the sensorimotor fingerprint in tremor disorders. There is a great overlap in the sensorimotor and tremor networks leading to several limitations. First, subtle differences in tremor-related areas could have been overruled by vigorous task-related activity. More subtle cerebellar tasks might provide additional results. Second, brain networks and network functions in general are intertwined, and although there is no better alternative, investigating both the sensorimotor network and the tremor network in one design assumes a potentially artificial separation. From the obtained within-group results, we concluded that there was also an overlap between the efferent motor areas and the afferent sensory areas. The isolated motor contrast (active>passive) that theoretically revealed the motor network separating it from the sensory network showed cortical sensory areas as well, although most areas contributed to motor output. Third, because tremor in both groups reveal itself overall in different conditions (rest vs. action), we could not make a direct comparison with identical regressors. However, the latter is also a strength of our design, as it allows us to analyze tremor-related areas, separately from the conditions, with help of a tremor regressor that is orthogonalized with respect to the tasks providing a measure of specific additional tremor

fluctuations. We believe that the tremor-related activity that occurred in rest and action in the PD and ET patients, respectively, provides a representative derivation of tremor amplitude fluctuation.

Despite the above-mentioned limitations, this novel approach including a wrist manipulator enables sensorimotor investigation in a novel controlled manner. This design may be a stepping stone towards a diagnostic and/or therapeutic use in tremor disorders.

5. Conclusion

By perturbing the sensorimotor loop with a novel MR-compatible wrist manipulator, specific sensorimotor fingerprints of tremor disorders can be identified. In ET, sensorimotor network function related to intentional movements does not seem be affected, in contrast to PD. Focusing on tremor related activations within the sensorimotor network, our findings suggest that the cerebellum seems to play a role in tremor modulation in PD while the inferior olive does so in ET.

Funding sources

Supplementary material

Fig. 1. A. Visual instructions as presented to the participant. (A) The visual cue for the rest and passive condition. The red cross indicates that no torque is required. The green circle and black crosshairs will be static during the task (B) The visual cue for the active condition. The participant is asked to apply torque to keep the black crosshair inside the green circle. The black crosshair indicates the position compared to the reference, providing visual feedback.

Fig. 2. A. Photograph (WM) of the complete system prototype. Indicated are the real-time computer,electro-motor and drive, hydraulic pump, reservoir and valves, 2×9 meter tube, emergency stop button, vane motor and the optical sensors.

Fig. 3. A. (A) Schematic display of the experimental setup. (B) The subject was in supine position inside the bore of the MRI scanner with the right arm attached to a handle beside the body. Figure adapted from Vlaar et al. (2016).

Fig. 4. A. An example of a task block design; GLM includes three conditions each 30 s (active, passive and rest), the instruction blocks (5 s) of the active and passive movement conditions and the movement parameters.

Fig. 5. A. An example of a tremor block design; GLM includes three conditions each 30 s (active, passive and rest), the instruction blocks (5 *s*) of the active and passive movement conditions, EMG regressor and the movement parameters.

Fig. 6. A. Sensorimotor mask used for within group analyses (total of 44,751 voxels). Including primary motor cortex, primary somatosensory cortex, sensorimotor association areas (premotor cortex (brodmann area 6) and secondary sensory areas (operculum), cerebellum (anterior lobe and lobule VIII), basal ganglia and thalamus.

Data Availability

Data will be made available on request.

Credit authorship contribution statement

S. Sharifi: Conceptualization, Methodology, Investigation, Formal analysis, Data curation, Visualization, Writing – original draft, Writing – review & editing. **F. Luft:** Conceptualization, Investigation, Data curation, Writing – review & editing. **L. de Boer:** Methodology, Investigation, Formal analysis, Data curation, Writing – review & editing. **A.W.G. Buijink:** Methodology, Formal analysis, Data curation, Writing – review & editing. **W. Mugge:** Conceptualization, Methodology, Data curation, Writing – review & editing. **A.C. Schouten:** Conceptualization, Methodology, Data curation, Writing – review & editing. **T. Heida:** Conceptualization, Methodology, Data curation, Writing – review & editing. **L.J. Bour:** Conceptualization, Methodology, Data curation, Writing – review & editing. **A.F. van Rootselaar:** Conceptualization, Methodology, Formal analysis, Data curation, Writing – original draft, Writing – review & editing.

Acknowledgments

Supplementary materials

Supplementary material associated with this article can be found, in the online version, at doi:10.1016/j.neuroimage.2022.119554.

References

Armstrong, M.J., Okun, M.S., 2020. Diagnosis and treatment of parkinson disease: a review. JAMA 323, 548–560. doi:10.1001/JAMA.2019.22360.

Bain, P., Brin, M., Deuschl, G., Elble, R., Jankovic, J., Findley, L., Koller, W.C., Pahwa, R., 2000. Criteria for the diagnosis of essential tremor. Neurology 54, S7.

Beissner, F., Schumann, A., Brunn, F., Eisenträger, D., Bär, K.J., 2014. Advances in functional magnetic resonance imaging of the human brainstem. Neuroimage 86, 91–98. doi:10.1016/j.neuroimage.2013.07.081.

Bode, D., Mugge, W., Schouten, A.C., van Rootselaar, A.-.F., Bour, L.J., van der Helm, F.C.T., Lammertse, P., 2017. Design of a magnetic resonance-safe haptic wrist manipulator for movement disorder diagnostics. J. Med. Device 11. doi:10.1115/1.4037674.

Boecker, H., Weindl, A., Brooks, D.J., Ceballos-Baumann, A.O., Liedtke, C., Miederer, M., Sprenger, T., Wagner, K.J., Miederer, I., 2010. GABAergic dysfunction in essential tremor: an 11C-flumazenil PET study. J. Nucl. Med. 51, 1030–1035. doi:10.2967/jnumed.109.074120.

Boecker, H., Wills, A.J., Ceballos-Baumann, A., Samuel, M., Thompson, P.D., Findley, L.J., Brooks, D.J., 1996. The effect of ethanol on alcohol-responsive essential tremor: a positron emission tomography study. Ann. Neurol. 39, 650–658. doi:10.1002/ana.410390515.

Brooks, J.C.W., Faull, O.K., Pattinson, K.T.S., Jenkinson, M., 2013. Physiological noise in brainstem fMRI. Front. Hum. Neurosci. 0, 623. doi:10.3389/FN-HUM.2013.00623/BIBTEX.

Bucher, S.F., Seelos, K.C., Dodel, R.C., Reiser, M., Oertel, W.H., 1997. Activation mapping in essential tremor with functional magnetic resonance lmagng. Ann. Neurol. doi:10.1002/ana.410410108.

Buijink, Broersma, M., van der Stouwe, A.M.M., van Wingen, G.A., Groot, P.F.C., Speelman, J.D., Maurits, N.M., van Rootselaar, A.F., 2015a. Rhythmic finger tapping reveals cerebellar dysfunction in essential tremor. Park. Relat. Disord. 21, 383–388. doi:10.1016/j.parkreldis.2015.02.003.

Buijink, A.W.G., Van Der Stouwe, A.M.M., Broersma, M., Sharifi, S., Groot, P.F.C., Speelman, J.D., Maurits, N.M., Van Rootselaar, A.F., 2015b. Motor network disruption in essential tremor: a functional and effective connectivity study. Brain 138, 2934–2947. doi:10.1093/brain/awv225.

Caballero-Gaudes, C., Reynolds, R.C., 2017. Methods for cleaning the BOLD fMRI signal. Neuroimage 154, 128–149. doi:10.1016/j.neuroimage.2016.12.018.

Coenen, V.A., Rijntjes, M., Prokop, T., Piroth, T., Amtage, F., Urbach, H., Reinacher, P.C., 2016. One-pass deep brain stimulation of dentato-rubro-thalamic tract and subthalamic nucleus for tremor-dominant or equivalent type Parkinson's disease. Acta Neurochir. 158, 773–781. doi:10.1007/s00701-016-2725-4, (Wien).

Colebatch, J.G., Frackowiak, R.S.J., Brooks, D.J., Colebatch, J.G., Findley, L.J., Marsden, C.M., 1990. Preliminary report: activation of the cerebellum in essential tremor. Lancet 336, 1028–1030. doi:10.1016/0140-6736(90)92489-5.

DeLong, M.R., Wichmann, T., 2007. Circuits and circuit disorders of the basal ganglia. Arch. Neurol. 64, 20–24. doi:10.1001/ARCHNEUR.64.1.20.

Dirkx, M.F., Bologna, M., 2022. The pathophysiology of Parkinson's disease tremor. J. Neurol. Sci. 435, 120196. doi:10.1016/j.jns.2022.120196.

Dirkx, M.F., den Ouden, H., Aarts, E., Timmer, M., Bloem, B.R., Toni, I., Helmich, R.C., 2016. The cerebral network of parkinson's tremor: an effective connectivity fMRI study. J. Neurosci. 36, 5362–5372. doi:10.1523/JNEUROSCI.3634-15.2016.

Eickhoff, S.B., Paus, T., Caspers, S., Grosbras, M.H., Evans, A.C., Zilles, K., Amunts, K., 2007. Assignment of functional activations to probabilistic cytoarchitectonic areas revisited. Neuroimage 36, 511–521. doi:10.1016/j.neuroimage.2007.03.060.

Elble, R., Comella, C., Fahn, S., Hallett, M., Jankovic, J., Juncos, J.L., Lewitt, P., Lyons, K., Ondo, W., Pahwa, R., Sethi, K., Stover, N., Tarsy, D., Testa, C., Tintner, R., Watts, R., Zesiewicz, T., 2012. Reliability of a new scale for essential tremor. Mov. Disord. 27, 1567–1569. doi:10.1002/mds.25162.

Friston, K., Holmes, A., Worsley, K., Poline, J., Frith, C., Frackowiak, R., 1995. Statistical parametric maps in functional imaging: a general linear approach. Hum. Brain Mapp 2, 189.

Gallea, C., Popa, T., García-Lorenzo, D., Valabregue, R., Legrand, A.P., Marais, L., Degos, B., Hubsch, C., Fernández-Vidal, S., Bardinet, E., Roze, E., Lehéricy, S., Vidailhet, M., Meunier, S., 2015. Intrinsic signature of essential tremor in the cerebellofrontal network. Brain 138, 2920–2933. doi:10.1093/brain/awv171.

Goetz, C.G., Tilley, B.C., Shaftman, S.R., Stebbins, G.T., Fahn, S., Martinez-Martin, P., Poewe, W., Sampaio, C., Stern, M.B., Dodel, R., Dubois, B., Holloway, R., Jankovic, J., Kulisevsky, J., Lang, A.E., Lees, A., Leurgans, S., LeWitt, P.A., Nyenhuis, D., Olanow, C.W., Rascol, O., Schrag, A., Teresi, J.A., van Hilten, J.J., LaPelle, N., Agarwal, P., Athar, S., Bordelan, Y., Bronte-Stewart, H.M., Camicioli, R., Chou, K., Cole, W., Dalvi, A., Delgado, H., Diamond, A., Dick, J.P., Duda, J., Elble, R.J., Evans, C., Evidente, V.G., Fernandez, H.H., Fox, S., Friedman, J.H., Fross, R.D., Gallagher, D., Goetz, C.G., Hall, D., Hermanowicz, N., Hinson, V., Horn, S., Hurtig, H., Kang, U.J., Kleiner-Fisman, G., Klepitskaya, O., Kompoliti, K., Lai, E.C., Leehey, M.L., Leroi, I., Lyons, K.E., McClain, T., Metzer, S.W., Miyasaki, J., Morgan, J.C., Nance, M., Nemeth, J., Pahwa, R., Parashos, S.A., Schneider, J.S.J.S., Schrag, A., Sethi, K., Shulman, L.M., Siderowf, A., Silverdale, M., Simuni, T., Stacy, M., Stern, M.B., Stewart, R.M., Sullivan, K., Swope, D.M., Wadia, P.M., Walker, R.W., Walker, R., Weiner, W.J., Wiener, J., Wilkinson, J., Wojcieszek, J.M., Wolfrath, S., Wooten, F., Wu, A., Zesiewicz, T.A., Zweig, R.M., 2008. Movement disorder society-sponsored revision of the unified Parkinson's disease rating scale (MDS-UPDRS): scale presentation and clinimetric testing results. Mov. Disord. 23, 2129–2170. doi:10.1002/mds.22340.

Goldman, R.I., Stern, J.M., Engel, J., Cohen, M.S., 2000. Acquiring simultaneous EEG and functional MRI. Clin. Neurophysiol. 111, 1974–1980. doi:10.1016/S1388-2457(00)00456-9.

Hallett, M., Dubinsky, R.M., 1993. Glucose metabolism in the brain of patients with essential tremor. J. Neurol. Sci. 114, 45–48. doi:10.1016/0022-510X(93)90047-3.

Helmich, R.C., Janssen, M.J.R.R., Oyen, W.J.G.G., Bloem, B.R., Toni, I., 2011. Pallidal dysfunction drives a cerebellothalamic circuit into Parkinson tremor. Ann. Neurol. 69, 269–281. doi:10.1002/ana.22361.

Holtbernd, F., Shah, N.J., 2021. Imaging the Pathophysiology of essential tremor—a systematic review. Front. Neurol. 12, 856. doi:10.3389/FNEUR.2021.680254/BIBTEX.

Jain, S., Lo, S.E., Louis, E.D., 2006. Common misdiagnosis of a common neurological disorder: how are we misdiagnosing essential tremor? Arch. Neurol. 63, 1100–1104. doi:10.1001/archneur.63.8.1100.

Kühn, A.A., Kupsch, A., Schneider, G.H., Brown, P., 2006. Reduction in subthalamic 8–35 Hz oscillatory activity correlates with clinical improvement in Parkinson's disease. Eur. J. Neurosci. 23, 1956–1960. doi:10.1111/J.1460-9568.2006.04717.X.

León, J.B., Gironell, A., De La, H., Creu, S., Pau, S., Benito, S., Alonso, C., Holtbernd, F., Shah, N.J., 2021. Imaging the pathophysiology of essential tremor-a systematic review. Front. Neurol. 1, 680254. doi:10.3389/fneur.2021.680254. www.frontiersin.org.

Li, J.Y., Lu, Z.J., Suo, X.L., Li, N.N., Lei, D., Wang, L., Peng, J.X., Duan, L.R., Xi, J., Jiang, Y., Gong, Q.Y., Peng, R., 2020. Patterns of intrinsic brain activity in essential tremor with resting tremor and tremor-dominant Parkinson's disease. Brain Imaging Behav. 14 (6), 2606–2617. doi:10.1007/s11682-019-00214-4, PMID: 31989422.

Liu, T.T., Nalci, A., Falahpour, M., 2017. The global signal in fMRI: nuisance or Information? Neuroimage 150, 213–229. doi:10.1016/j.neuroimage.2017.02.036.

Louis, E.D., 2016. Essential tremor: a common disorder of purkinje neurons? Neuroscientist 22, 108–118. doi:10.1177/1073858415590351.

Louis, E.D., Lenka, A., 2017. The olivary hypothesis of essential tremor: time to lay this model to rest? Tremor Other Hyperkinet. Mov. 7, 473. doi:10.7916/D8FF40RX, (N. Y).

Louis, E.D., Machado, D.G., 2015. Tremor-related quality of life: a comparison of essential tremor vs. Parkinson's disease patients. Parkinsonism Relat. Disord. 21, 729–735. doi:10.1016/J.PARKRELDIS.2015.04.019.

Miwa, H., 2007. Rodent models of tremor. Cerebellum doi:10.1080/14734220601016080.

Murphy, K., Fox, M.D., 2017. Towards a consensus regarding global signal regression for resting state functional connectivity MRI. Neuroimage 154, 169–173. doi:10.1016/j.neuroimage.2016.11.052.

Nambu, A., Tokuno, H., Takada, M., 2002. Functional significance of the cortico–subthalamo–pallidal 'hyperdirect' pathway. Neurosci. Res. 43, 111–117. doi:10.1016/S0168-0102(02)00027-5.

Neely, K.A., Kurani, A.S., Shukla, P., Planetta, P.J., Shukla, A.W., Goldman, J.G., Corcos, D.M., Okun, M.S., Vaillancourt, D.E., 2015. Functional brain activity relates to 0-3 and 3-8 Hz force oscillations in essential tremor. Cereb. Cortex 25, 4192–4202. doi:10.1093/cercor/bhu142.

Nichols, T.E., Holmes, A.P., 2002. Nonparametric permutation tests for functional neuroimaging: a primer with examples. Hum. Brain Mapp. 15, 1–25. doi:10.1002/hbm.1058.

Novaes, N.P., Balardin, J.B., Hirata, F.C., Melo, L., Amaro, E., Barbosa, E.R., Sato, J.R., Cardoso, E.F., 2021. Global efficiency of the motor network is decreased in Parkinson's disease in comparison with essential tremor and healthy controls. Brain Behav. 11, e02178. doi:10.1002/BRB3.2178.

Park, Y.G., Park, H.Y., Lee, C.J., Choi, S., Jo, S., Choi, H., Kim, Y.H., Shin, H.S., Llinas, R.R., Kim, D., 2010. Ca(V)3.1 is a tremor rhythm pacemaker in the inferior olive. Proc. Natl. Acad. Sci. U. S. A. doi:10.1073/pnas.1002995107.

Pollok, B., Makhloufi, H., Butz, M., Gross, J., Timmermann, L., Wojtecki, L., Schnitzler, A., 2009. Levodopa affects functional brain networks in parkinsonian resting tremor. Mov. Disord. 24, 91–98. doi:10.1002/MDS.22318.

Power, J.D., Barnes, K.A., Snyder, A.Z., Schlaggar, B.L., Petersen, S.E., 2013. Steps toward optimizing motion artifact removal in functional connectivity MRI; a reply to carp. Neuroimage doi:10.1016/j.neuroimage.2012.03.017.

Power, J.D., Schlaggar, B.L., Petersen, S.E., 2015. Recent progress and outstanding issues in motion correction in resting state fMRI. Neuroimage 105, 536–551. doi:10.1016/j.neuroimage.2014.10.044.

Prent, N., Potters, W.V., Boon, L.I., Caan, M.W.A., de Bie, R.M.A., van den Munckhof, P., Schuurman, P.R., van Rootselaar, A.F., 2020. Distance to white matter tracts is associated with deep brain stimulation motor outcome in Parkinson's disease. J. Neurosurg. 433–442. doi:10.3171/2019.5.JNS1952.

Rizzo, G., Copetti, M., Arcuti, S., Martino, D., Fontana, A., Logroscino, G., 2016. Accuracy of clinical diagnosis of Parkinson disease. Neurology 86, 566–576. doi:10.1212/WNL.0000000000002350.

Rolls, E.T., Huang, C.C., Lin, C.P., Feng, J., Joliot, M., 2020. Automated anatomical labelling atlas 3. Neuroimage 206, 116189. doi:10.1016/J.NEUROIMAGE.2019.116189.

Rowland, N.C., de Hemptinne, C., Swann, N.C., Qasim, S., Miocinovic, S., Ostrem, J., Knight, R.T., Starr, P.A., 2015. Task-related activity in sensorimotor cortex in Parkinson's disease and essential tremor: changes in beta and gamma bands. Front. Hum. Neurosci. 0, 512. doi:10.3389/FNHUM.2015.00512.

Sahyoun, C., Floyer-Lea, A., Johansen-Berg, H., Matthews, P.M., 2004. Towards an understanding of gait control: brain activation during the anticipation, preparation and execution of foot movements. Neuroimage 21, 568–575. doi:10.1016/j.neuroimage.2003.09.065.

Schouten, A.C., Mugge, W., 2018. Closed-loop identification to unravel the way the human nervous system controls bodily functions. Biosyst. Biorobotics 21, 617–621. doi:10.1007/978-3-030-01845-0_123.

Schrag, A., Münchau, A., Bhatia, K.P., Quinn, N.P., Marsden, C.D., 2000. Essential tremor: an overdiagnosed condition? J. Neurol. 247, 955–959. doi:10.1007/s004150070053.

Sharifi, S., Nederveen, A.J., Booij, J., Van Rootselaar, A.F., 2014. Neuroimaging essentials in essential tremor: a systematic review. NeuroImage Clin. 5, 217–231. doi:10.1016/j.nicl.2014.05.003.

Spraker, M.B., Prodoehl, J., Corcos, D.M., Comella, C.L., Vaillancourt, D.E., 2010. Basal ganglia hypoactivity during grip force in drug naïve Parkinson's disease. Hum. Brain Mapp. 31, 1928. doi:10.1002/HBM.20987.

Timmermann, L., Gross, J., Dirks, M., Volkmann, J., Freund, H.J., Schnitzler, A., 2003. The cerebral oscillatory network of parkinsonian resting tremor. Brain 126, 199–212. doi:10.1093/brain/awg022.

van der Meer, J.N., Tijssen, M.A.J., Bour, L.J., van Rootselaar, A.F., Nederveen, A.J., 2010. Robust EMG-fMRI artifact reduction for motion (FARM). Clin. Neurophysiol. 121, 766–776. doi:10.1016/j.clinph.2009.12.035.

van der Stouwe, A.M.M., Nieuwhof, F., Helmich, R.C., 2020. Tremor pathophysiology: lessons from neuroimaging. Curr. Opin. Neurol. 33, 474–481. doi:10.1097/WCO.0000000000000829.

Van Rootselaar, A.F., Maurits, N.M., Renken, R., Koelman, J.H.T.M., Hoogduin, J.M., Leenders, K.L., Tijssen, M.A.J., 2008. Simultaneous EMG-functional MRI recordings can directly relate hyperkinetic movements to brain activity. Hum. Brain Mapp. doi:10.1002/hbm.20477.

Vlaar, M.P., Mugge, W., Groot, P.F.C., Sharifi, S., Bour, L.J., van der Helm, F.C.T., van Rootselaar, A.F., Schouten, A.C., 2016. Targeted brain activation using an MR-compatible wrist torque measurement device and isometric motor tasks during functional magnetic resonance imaging. Magn. Reson. Imaging 34, 795–802. doi:10.1016/j.mri.2016.02.002.

Weiller, C., Jüptner, M., Fellows, S., Rijntjes, M., Leonhardt, G., Kiebel, S., Müller, S., Diener, H.C., Thilmann, A.F., 1996. Brain representation of active and passive movements. Neuroimage (4) 105–110. doi:10.1006/nimg.1996.0034.